Whole bone mechanics and mechanical testing

Article *in* The Veterinary Journal · August 2008

DOI: 10.1016/j.tvjl.2007.09.012 · Source: PubMed

3 authors:

Amnon Sharir
University of California, San Francisco
30 PUBLICATIONS **1,632** CITATIONS
SEE PROFILE

Meir M Barak
Long Island University
29 PUBLICATIONS **503** CITATIONS
SEE PROFILE

Ron Shahar
Hebrew University of Jerusalem
136 PUBLICATIONS **2,682** CITATIONS
SEE PROFILE

Available online at www.sciencedirect.com
ScienceDirect
The Veterinary Journal 177 (2008) 8–17
The Veterinary Journal
www.elsevier.com/locate/tvjl

Review

Whole bone mechanics and mechanical testing

Amnon Sharir [a], Meir Max Barak [b], Ron Shahar [a,*]

[a] *Laboratory of Biomechanics, Koret School of Veterinary Medicine, The Hebrew University of Jerusalem, Rehovot 76100, Israel*
[b] *Department of Structural Biology, Weismann Institute of Science, Rehovot 76100, Israel*

Accepted 13 September 2007

Abstract

The mechanical behaviour of material bone can be completely described by a group of material properties. The mechanical behaviour of the entire bone organ, however, is much more difficult to predict; it is the result both of the properties of the material of which it is made, and of the geometric spatial architecture in which this is arranged.

This review first describes material bone in terms of its complex, graded and hierarchical structure. Basic concepts used in the field of mechanics of materials are defined and explained and then used to describe the mechanical properties of whole bone. Some clinical implications of these properties are provided. Commonly used mechanical testing methods for the study of the mechanical behaviour of whole bone are reviewed and the technical difficulties associated with them are discussed.

Keywords: Whole bone; Biomechanics; Structure; Graded structure; Bending

Introduction

Understanding the relationship between the mechanical responses of whole entities, their material properties and their shape, is a challenge. This is greatly enhanced when the material itself is complex, and when the entity it forms has a convoluted shape. This is almost always the case in biology. Despite major technical advances made in recent years in experimental techniques, we are still unable to predict and fully understand the mechanical functions of whole biological entities such as bones.

Various attempts have been made to address these objectives. These have been based mainly on mechanically measuring deformations of whole bones at a few individual locations (Burr et al., 1996; Milgrom et al., 2004), or developing constitutive theoretical models that can predict the behaviour of the whole bone based on the mechanical properties of its individual constituent materials (Silva et al., 2005). However due to limitations inherent in these methods, both approaches have, for the most part, only been partially successful; single-point strain measurements (the concept of 'strain' is defined in detail below) miss local variations that are extremely significant in a complex structure such as whole bone, while the accuracy of numerical models relies on knowledge of the material properties that is not available. Recent advances in optical metrology have opened up new opportunities as they enable the precise and accurate mapping of the manner in which the *entire surface* of a whole bone deforms.

Detailed data describing the displacement maps of the entire surface of bones create the exciting possibility of relating the complex distribution of mechanical properties of loaded bone and its microstructures to deformations and strains. Such studies could improve our understanding of normal physiological processes, such as skeletal aging, as well as disease processes such as osteoporosis. They also provide opportunities for engineers designing bio-inspired materials to study the principles, advantages and characteristics of the behaviour of hierarchical and multifunctional materials (Gao, 2006; Mayer, 2005). In this review we shall describe the material bone, introduce the basic terms used

* Corresponding author. Tel.: +972 8 9489756; fax: +972 8 9467940.
E-mail address: Shahar@agri.huji.ac.il (R. Shahar).

1090-0233/$ - see front matter © 2007 Elsevier Ltd. All rights reserved.
doi:10.1016/j.tvjl.2007.09.012

when describing mechanics of bones, and describe the methods commonly used to test the mechanical performance of whole bone.

The material bone

'Bone' is a term used to describe both the organ bone and the material it is made of. The material of all bones has the same constituents. These include mineral, carbonated hydroxyapatite (also known as dahllite), the framework protein type I collagen, many other so-called non-collagenous proteins and water (Delmas et al., 1984).

The material of bones has a hierarchical structure that changes at different length scales (Fig. 1). It is also a graded material, as its composition, structure, and mechanical properties may vary continuously or in discrete steps from one location to another (Suresh, 2001). The combination of these two attributes results in a very complex material type that certainly can not be described in terms of a single value for a particular materials property. The following is a brief description of the different hierarchies of bone (the material), and its graded nature.

The hierarchical structure of bone

The various hierarchies of bone span many different length scales. The basic building blocks of the material bone are an organic matrix, most of which is type-I collagen, and a mineral phase (level 1, Fig. 1) (Weiner and Wagner, 1998). At a higher length scale bone is composed of mineralised collagen fibrils 80–100 nm in diameter (level 2, Fig. 1), arranged in a regular, staggered array of collagen molecules (level 3, Fig. 1) (Hodge and Petruska, 1963). The crystals are located within and around these fibrils. They are about 50 nm long, 25 nm wide and 2–3 nm thick (Fratzl et al., 1996; Weiner and Wagner, 1998). At the next hierarchical level, the mineralised fibrils are organised in a variety of patterns, the most common of which is the lamella (level 4, Fig. 1). Each lamella is 2–3 μm thick and is arranged in several discrete layers of parallel fibrils, each layer having a different orientation of fibrils. A similar arrangement can be found in plywood, and is therefore referred to as the *rotated plywood motif* (Weiner et al., 1999).

At the next hierarchical level, lamellae are arranged in one of several possible ways, depending on location and species; in mature equine and canine bone the most common arrangement is concentric layers (called secondary osteons or Haversian systems). These form cylinders 150–250 μm in diameter and contain a central hollow tube ~80 μm in diameter, which contains blood vessels and nerves (level 5, Fig. 1) (Currey, 2002). Other common forms include fibrolamellar bone (also known as plexiform, such as much of bovine bone), and lamellar-zonal bone (as in the long bones of reptiles). At the next level, bone can be mostly solid (cortical) or sponge-like (cancellous) with numerous voids separating thin struts and plates (trabecu-

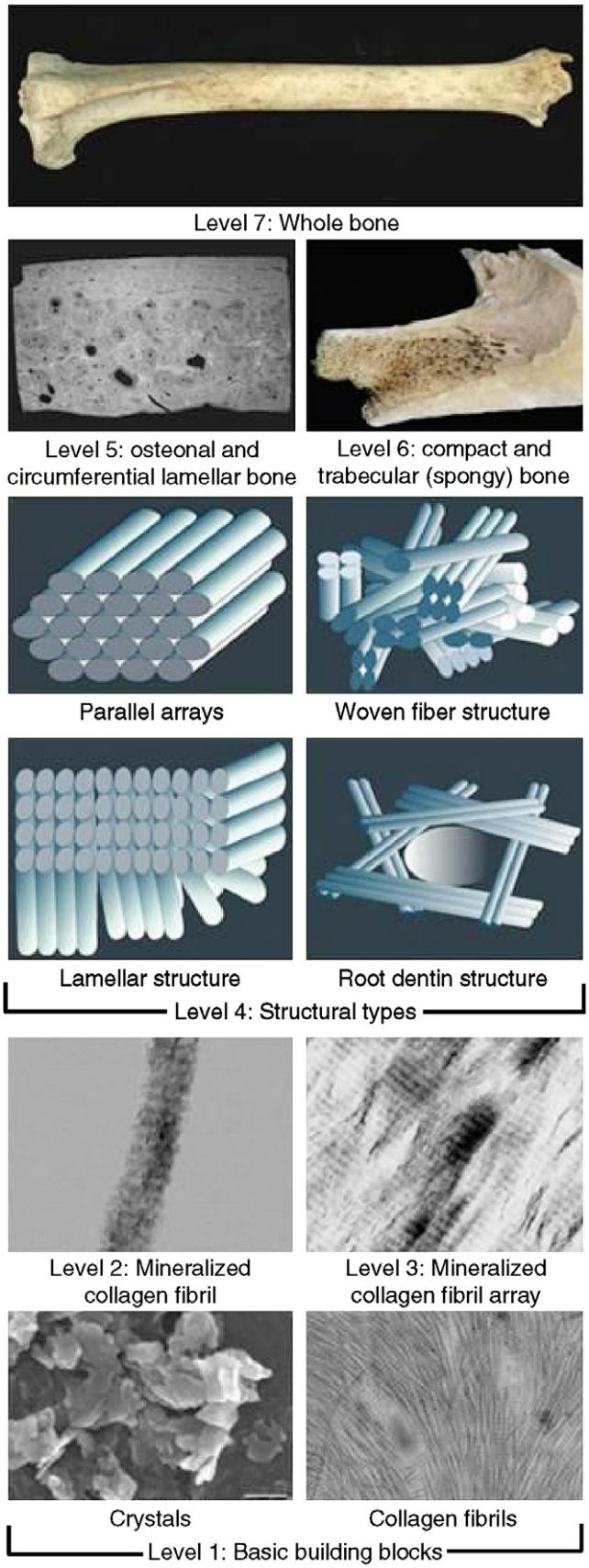

Fig. 1. The hierarchical levels of organisation of bone (provided by Professor Steve Weiner of the Weizmann Institute of Science, Rehovot, Israel).

lae) (level 6, Fig. 1). This entire complex arrangement, with different but characteristic three-dimensional (3D) geometric morphology, ultimately forms the organ bone.

The graded structure of bone material

The mechanical response of materials with spatial gradients in composition and structure is of considerable interest in diverse disciplines such as tribology, geology, optoelectronics, biomechanics, fracture mechanics and nanotechnology (Suresh, 2001). The damage and failure resistance of surfaces to normal and shear contact or impact can be changed substantially through such gradients. The composition, structure, and mechanical properties of a material may vary either continuously or in discrete steps with depth beneath a free surface. Gradations in microstructure and/or porosity are commonly seen in biological structures such as plant stems and bone, where the strongest elements are located in regions that experience the highest stresses. Learning from nature, materials scientists increasingly aim to engineer graded materials that are more damage-resistant than their conventional homogeneous counterparts (Mayer, 2005). This is particularly important on surfaces or at interfaces between dissimilar materials, for example orthopaedic implants, where contact failure commonly occurs.

Bone is a prime example of a naturally-occurring graded material. The graded structure of bone can be seen at several levels. At the osteonal level, for example, differences in the level of mineralisation occur within osteons, since the inner (younger) lamellae are initially less mineralised than the outer lamellae; at a later time they become more mineralised because they are closer to the blood supply. Furthermore, the outer border of an osteon (so-called cement line) is believed to contain very little collagen (Currey, 2002), however its mineral content is still unclear; while some authors report that it has a higher mineral content than the surrounding bone (Frasca, 1981), others claim it has much lower mineral content (Schaffler et al., 1989). Another example is the so-called interstitial lamellae (remnants of old osteons) which occupy regions between intact osteons, which are more highly mineralised than the osteons. This graded structure critically affects the mechanical behaviour of bone, and in particular crack propagation. As most cracks tend to advance until reaching cement lines, at which point they stop due to this weak interface and travel around the osteon rather than through it (Taylor and Lee, 2003). At another level, the transition between cortical and cancellous bone is also graded, and can be observed grossly in terms of increasing bone porosity from the periosteal to the endosteal surface.

Basic concepts of mechanics of materials

The mechanical behaviour of a structure is determined by its geometry and the properties of the material (or materials) of which it is made. The material properties are independent of the geometry and are inherent to the material itself. The determination of these properties requires definition of the concepts 'stress' and 'strain'. The following is a short, and by no means rigorous or complete, description of these concepts. Further information can be found in texts on the theory of elasticity (such as Fung and Tong, 2001); brief bone-oriented summaries can be found in the excellent texts by Martin et al. (1998), Cowin (2001) and Currey (2002).

Stress

The intuitive explanation of the concept of stress is load per unit area, as shown in Fig. 2. When more rigorously defined, stress is a much more complex entity. When a three-dimensional body of arbitrary geometry is loaded (see Fig. 3a), one can imagine the body to be divided into numerous infinitely small cubes. Consider now one such cube somewhere within the body (see Fig. 3b). Each face will have a force acting upon it, which can be divided into three Cartesian components: one normal to the face and two parallel to it. The normal stress acting on this particular cube is defined as the normal force divided by the face area (both are infinitely small, but the ratio is finite).

The shear stresses are the ratios of the parallel forces divided by the same face area (see Fig. 3c), thus each face is subjected to three stress components. Each cube has six faces, thus the total number of stress components acting on the entire cube is 18. However, due to equilibrium requirements (opposite faces must have equal and opposite forces) the entire cube stress state can be described by nine components (three orthogonal faces with three components each). Symmetry considerations can be shown to further decrease the different shear components from six to three, so that the number of independent stress components is six (three normal stresses and three shear components). The magnitude of these components depends on the location of the cube. The mathematical entity described by six components is termed a second-degree tensor (scalars like mass and temperature are zero-degree tensors, and a vector like force is a first-degree tensor, described by three components). The units of stress are force over area, and the most common unit is the pascal (Pa) which is equal to 1 newton over 1 m^2 (N/m^2). One pascal represents a very small amount of stress, and since physiological stresses are usually in the range of thousands of Pa, a commonly used

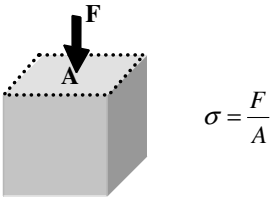

Fig. 2. Intuitive depiction of the concept of stress σ. F stands for the normal force applied, and A the cross-sectional area upon which this force acts.

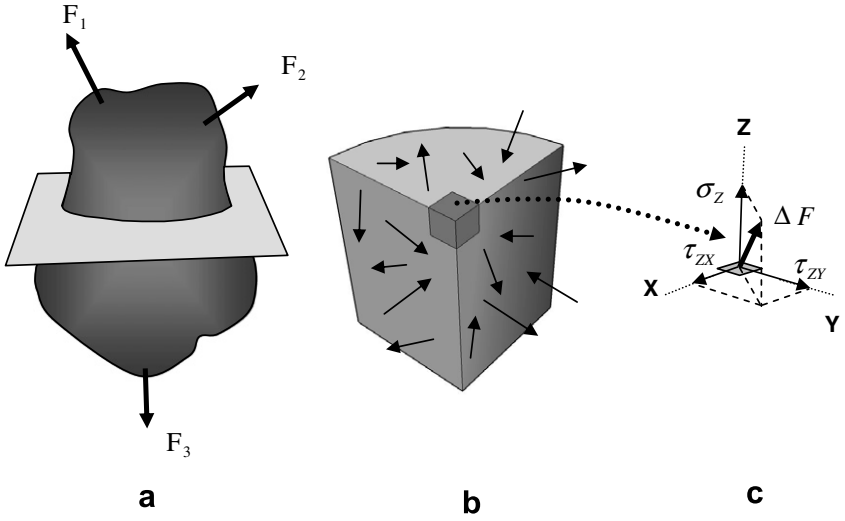

Fig. 3. (a) A body of arbitrary shape loaded by three external forces, in equilibrium. A horizontal plane is shown to cut the body at an arbitrary height. (b) The body is cut at an arbitrary point by *three* orthogonal planes which are identified by the direction normal to them (x, y and z). Internal forces act at each point on the cut surfaces (arrows). (c) The z-surface of an infinitesimal cube at the corner of the three planes, on which a force ΔF of arbitrary direction and magnitude is acting. This force can be divided into a normal component (creating a normal stress component σ_z at that point) and two in-plane components (creating two shear stress components τ_{zx} and τ_{zy} at that point).

unit is the megapascal (MPa), which is equal to 1,000,000 Pa.

Strain

Strain is another tensorial entity required to describe the mechanical behaviour of materials. Again, in an intuitive sense, strain signifies the fractional change in length of a loaded body. When one considers the same infinitely small cube within a loaded body as above, it can be seen that it may change its three dimensions along the length of each axis (normal strain) or change the angle between its faces (shear strain), as shown in Fig. 4a and Fig. 4b. Similar to stress, it can be shown that there are six independent strain tensor components (three normal strains, and three shear strains).

Strain is a unitless ratio (length over length), but is commonly measured in units of microstrain, so that a strain of 0.01 (1%) would be 10,000 microstrain. One of the most striking findings of bone biology is the fact that in *all* bones and in *all* animals the level of maximum physiological strain occurring in extreme activity (such as fast galloping) is within relatively narrow bounds, usually ranging between 1500 and 3000 microstrain (Currey, 2002). An exception was noted in fast-galloping race horses, in which compressive strains as high as 7862 microstrain were measured on the third metacarpal bone of a yearling at a treadmill speed of 16.5 m/s (Davies, 2005).

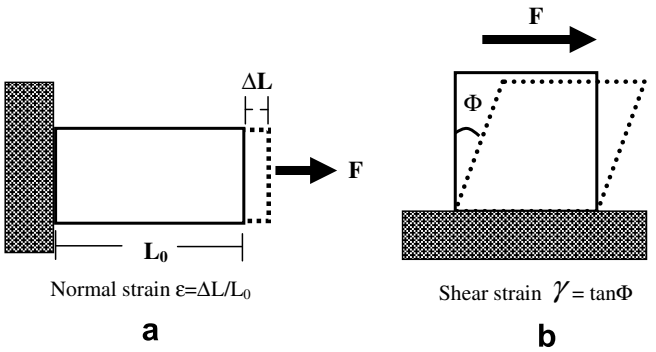

Fig. 4. (a) Normal strain ε and (b) Shear strain γ.

Stress–strain relationship

For so-called linearly elastic materials (to which bone belongs) the amount by which a material is deformed (strain) is linearly related to the force causing the deformation (stress). This relationship is called Hooke's law of elasticity. In its most general form, it states that each of the six stress components σ_i is equal to a linear combination of all six strain components ε_i through six constants of proportionality C_{ij}.

$$\begin{aligned}
\sigma_1 &= C_{11}\epsilon_1 + C_{12}\epsilon_3 + C_{13}\epsilon_3 + C_{14}\epsilon_4 + C_{15}\epsilon_5 + C_{16}\epsilon_6 \\
\sigma_2 &= C_{21}\epsilon_1 + C_{22}\epsilon_3 + C_{23}\epsilon_3 + C_{24}\epsilon_4 + C_{25}\epsilon_5 + C_{26}\epsilon_6 \\
\sigma_3 &= C_{31}\epsilon_1 + C_{32}\epsilon_3 + C_{33}\epsilon_3 + C_{34}\epsilon_4 + C_{35}\epsilon_5 + C_{36}\epsilon_6 \\
\sigma_4 &= C_{41}\epsilon_1 + C_{42}\epsilon_3 + C_{43}\epsilon_3 + C_{44}\epsilon_4 + C_{45}\epsilon_5 + C_{46}\epsilon_6 \\
\sigma_5 &= C_{51}\epsilon_1 + C_{52}\epsilon_3 + C_{53}\epsilon_3 + C_{54}\epsilon_4 + C_{55}\epsilon_5 + C_{56}\epsilon_6 \\
\sigma_6 &= C_{61}\epsilon_1 + C_{62}\epsilon_3 + C_{63}\epsilon_3 + C_{64}\epsilon_4 + C_{65}\epsilon_5 + C_{66}\epsilon_6
\end{aligned} \quad (1)$$

Thus, for the most general material there can be $6 \times 6 = 36$ such independent proportionality constants that describe its mechanical behaviour. Energy considerations further reduce this number to a still-considerable 21 independent elastic constants.

Fortunately, for most materials the number of proportionality constants is much smaller. For example, only

two constants are required to describe the mechanical behaviour of isotropic materials (materials which do not have preferred orientations, and behave the same in every direction). Cortical osteonal bone, which is considered to be transversely isotropic, has two types of orientations (axial direction parallel to the direction of the osteons and the group of directions orthogonal to the axial direction) and requires five constants to describe its elastic behaviour. In such a material Eq. (1) becomes much simpler, with many of the coefficients C_{ij} equal to 0.

When a sample of bone is incrementally loaded, its stress–strain curve initially exhibits a linear relationship between the stress and the strain (the elastic region). However at a particular stress (yield stress) further increase in load results in a non-linear deformation response where small additional loads produce a large strain increase as a result of accumulation of damage (microcracks) in the material and resulting decrease in its stiffness (Fig. 5). Bone is said to start to deform 'plastically' at that point. Further increase in load will eventually result in breakage of the sample, and the stress at which this happens is named the ultimate stress and represents the strength of the material. It should be noted that the above description refers to testing samples of the material bone, to determine their inherent properties. Whole bone testing (described later) examines the relationship between load and deformation, and is affected both by the material properties, as well as the geometry and architecture of the bone.

Young's modulus

In isotropic materials, Hooke's law becomes a very simplified version of Eq. (1), where Young's modulus (E) represents the ratio between the stress applied to a sample (σ) and the strain occurring to the sample as a result (ε):

$$\sigma = E\epsilon \tag{2}$$

Young's modulus can be determined by an experiment where a sample of the material is subjected to a load, and the strain and stress are determined concurrently. Young's modulus of the material is the slope of the linear portion of the stress–strain curve (see Fig. 5). Young's modulus represents the stiffness of the material; the higher its value, the stiffer the material – therefore, more force is needed to produce the same strain when compared to a less stiff material. For transversely isotropic materials this relationship depends on whether the sample is loaded in the axial direction (and the modulus is the axial modulus E_A) or the transverse direction (and the modulus is the transverse modulus E_T). Most studies found that the axial modulus of cortical bone is between 15,000 and 25, 000 MPa, (often denoted as 15–25 gigapascal, GPa), about two times higher than the transverse modulus.

It has also been shown that since cortical bone is viscoelastic to a certain degree, its stiffness is strain-rate dependent; when bone is loaded, as the strain rate increases, its stiffness also increases. This effect has been shown to be relatively small; an increase of the strain rate by a factor of 1000 will increase the Young's modulus by only 40% (Currey, 1988). Another area of research receiving a lot of attention recently is the so-called field of the fracture mechanics behaviour of bone. This aspect deals with the laws governing the propagation of cracks in bone, however its description is beyond the scope of this review.

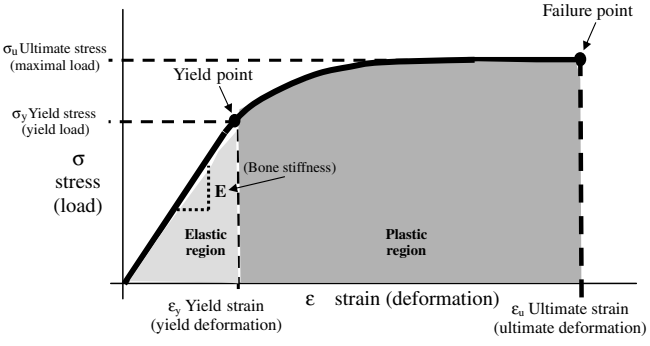

Fig. 5. The stress–strain curve obtained by loading a sample of compact bone in tension. E is the stiffness of the material (Young's modulus for isotropic materials). (Entities in parentheses represent results of whole bone experiments, in which the load–deformation relationship is described.)

Poisson's ratio

When a sample is loaded in compression, it becomes shorter in the load direction, but wider in the orthogonal direction. Similarly, when a sample is loaded in tension, it becomes longer but narrower (see Fig. 6). The negative ratio of the transverse strain component to the longitudinal strain component is called Poisson's ratio and is denoted by the letter υ. In most materials this ratio must be between 0 and 0.5; for bone it is usually between 0.1 and 0.33.

Mechanics of whole bones

Study of the mechanical performance of whole bones is clearly of much interest to researchers and clinicians alike.

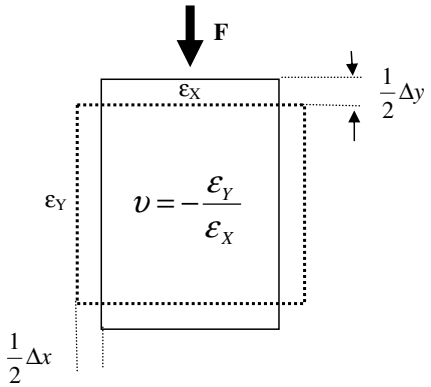

Fig. 6. Poisson's ratio υ: the negative ratio of the horizontal to vertical strain.

However, due to its complexity as described above, this is a most challenging and technically difficult endeavour. The stiffness of a structure (the extent to which it deforms under a particular load) depends on the type of loading, its geometry and on the mechanical properties of the materials of which it is made. This concept will be demonstrated using a structure which bears some resemblance to a long bone, namely a tube. When a tube is loaded in bending, one side undergoes tension while the other is loaded in compression (see Fig. 7). The interface between these two zones is under zero load, and is called the neutral axis. The stress at any point is given by

$$\sigma = \frac{Mc}{I} \tag{3}$$

where M is the applied bending moment, I is the cross-sectional moment of inertia and c is the distance of the chosen point from the neutral axis. I is a purely geometric entity, which for a tube-like structure depends only on the inner and outer diameters of the cross section of the tube. Substitution of σ from Eq. (3) yields the following relationship:

$$\epsilon = \frac{M \cdot C}{E \cdot I} \tag{4}$$

It is clear from Eq. (4) that the effectiveness of the tube to resist bending is directly related to E (the material stiffness) and the moment of inertia. Higher values of E or I decrease the strain (which is related to the deformation) of the structure. The cross-sectional moment of inertia of a tubular structure is given by

$$I = \frac{\pi}{4}(r_0^4 - r_i^4) \tag{5}$$

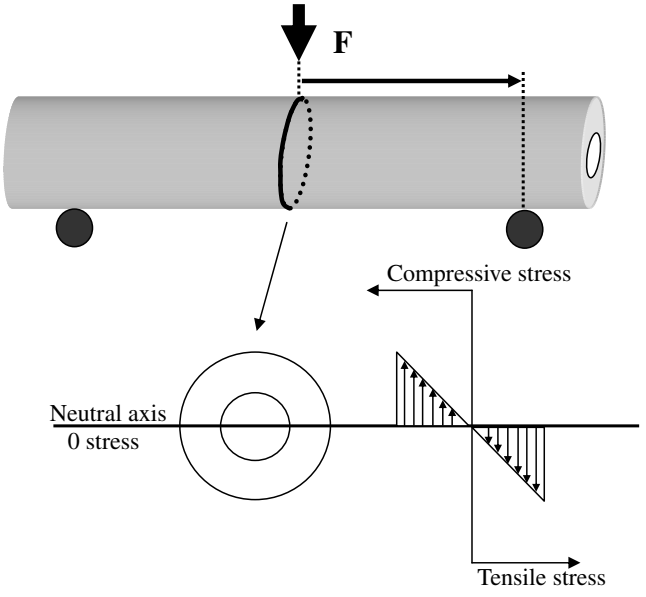

Fig. 7. 3-point bending of a tubular structure. The applied force F acts at the mid-point between the supports. The bottom half is loaded in tension, and the top half in compression, and the stress is zero at the middle (neutral axis). The horizontal stress increases linearly with the distance from the neutral axis.

where r_0 is the external radius and r_i is the internal radius. One consequence of Eqs. (4) and (5) is that if a tube undergoes modelling such that its inner radius increases more than the outer radius (as commonly happens during bone growth, resulting in its cortex becoming substantially thinner), the moment of inertia may still increase; therefore the stiffness of the new tube will *increase* despite having a thinner wall (see Fig. 8a).

To illustrate this point, let us assume that the femoral diaphysis of a young dog has a periosteal diameter of 15 mm and an endosteal diameter of 8 mm. Let us assume that as the dog matures the endosteal diameter increases by 38% (from 8 to 11 mm) and the periosteal diameter increases only by 7% (from 15 to 16 mm); this process will cause the thickness of the cortex to *decrease* from 3.5 mm to 2.5 mm. Yet the cross-sectional moment of inertia *increases* by 10%, as does the stiffness of the femoral diaphysis. It should be noted that these equations assume a simple and ideal geometric form, and bones are obviously not perfectly tubular structures. Nevertheless, these analytic expressions allow us to examine the mechanical behaviour of bones in an approximate manner.

Clinical implications

The following are two examples of the use of biomechanical principles to explain commonly-encountered clinical scenarios.

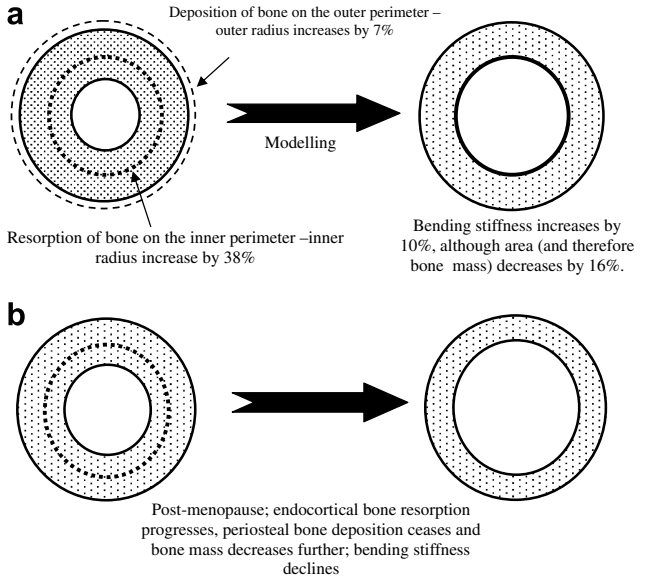

Fig. 8. (a) In young animals, modelling of long bones occurs primarily by resorption of the endosteal surface and bone deposition on the periosteal surface. Although the inner radius increases more than the outer radius (and the cortical thickness decreases) stiffness increases (because the moment of inertia is proportional to the difference of the radii to the 4th power). (b) During the post-menopausal period the rate of bone deposition decreases, and the moment of inertia decreases, and with it the bending stiffness.

Butterfly fragments

When viewing the radiographs of a fractured bone, the pattern of load it was subjected to can be figured out. This interpretation hinges upon the fact that the mechanical properties of the material bone, in particular its ultimate strength (the maximal load it can carry without breaking), depend on the mode of loading. Bone is stronger in compression compared to tension and weaker in shear (Turner, 2006). For instance, when a long bone is impact-loaded in a direction perpendicular to its long axis it bends, such that the side contacted by the impact is loaded in compression, while the opposite side is loaded in tension.

As a result, failure will begin on the opposite side to the impact (the tensile side) since it will reach its ultimate strength sooner than the side loaded in compression. As the advancing crack will reach the middle of the bone, it will reach compressed tissue, and due to bone's higher resistance to this type of load, it will advance in a path nearer to the bone's longitudinal direction, along the directions of maximal shear stress. In this way it will form a fracture with a so-called 'butterfly' fragment, commonly seen in practice (see Fig. 9).

Osteoporosis

Osteoporosis is one of the most common syndromes afflicting the aging human population, and in particular post-menopausal women. It is defined as a state of increased bone fracture risk, and is commonly linked to decreased estrogen levels. As a result, ovariohysterectomy is one of the most common methods to induce osteoporosis in animal models like mice and rats. The leading hypothesis for the observed increase in bone fragility is a combined effect of deterioration of the material properties (associated for instance with decreasing bone mineral density) and geometric changes. Geometric changes occur for instance when periosteal bone formation decreases while endosteal bone resorption increases or stays the same (Martin and Seeman, 2007). In pre-menopausal women endocortical bone resorption occurs and periosteal bone deposition compensates partly (see Fig. 8a). Therefore, since the moment of inertia is proportional to the 4th power of the distance of the material from the centre, resistance to bending may increase despite cortical thinning (an example was provided above). In the post-menopausal period, endocortical resorption accelerates while periosteal apposition slows down. Thus the cortices thin further and bending stiffness declines (see Fig. 8b).

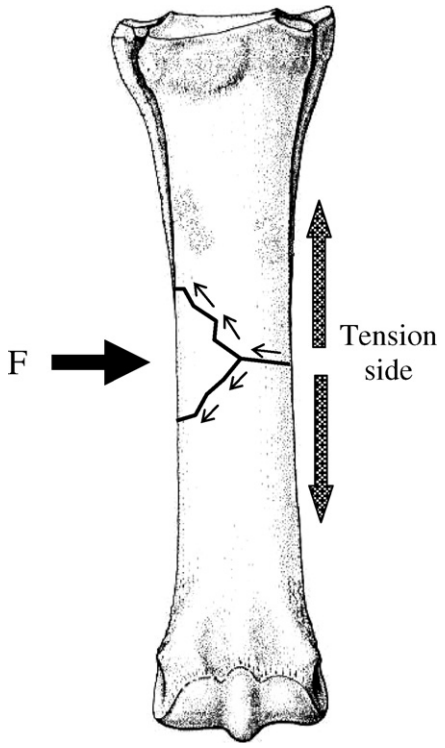

Fig. 9. Lateral impact loading of a long bone causes bending. The fracture starts at the tension side (away from the site of impact) and progresses across the bone up to the middle. When it reaches the compressive side, it 'runs' along the direction of maximal shear (at 45° to the transverse), creating a butterfly fragment.

Mechanical testing methods

Most investigations of the mechanical performance of whole bones rely on in vivo or in vitro experiments in which bones were tested in compression or by 3- or 4-point bending. Torsional loading and impact loading are also used, though less frequently. Measurements in these experiments consist of single values like load-to-yield and load-to-failure. Strain measurements are made at a very limited number of points (1–20) by placing strain gauges on the surface of bones. Alternatively, theoretical numerical models (mostly finite element models) which are based on numerous simplifying assumptions, particularly as far as material properties are concerned are used, and thus yield rough approximations only. In the last decade or so, the use of optical metrology to measure surface deformation has been reported, and offers several significant advantages. These methods will be described in detail in an upcoming paper. The following is a short description of mechanical testing methods of whole bones.

Bending

Bending tests are by far the most common methods used to test whole bones. They are used particularly to characterise the mechanical behaviour of bones of small experimental animals such as mice and rats belonging to different strains or treated by various drugs, which may affect the skeleton (Rubin and Lanyon, 1985; Robling et al., 2001; Ammann et al., 2003; Warden et al., 2005; Lane et al., 2006; Judex et al., 2007). Whole-bone bending tests are mostly 3-point or 4-point bending experiments. In 3-point bending the tested bone is positioned onto two supports, and a single-pronged loading device is applied to the opposite surface at a point precisely in the middle between the two supports (see Fig. 10a). In this loading regime

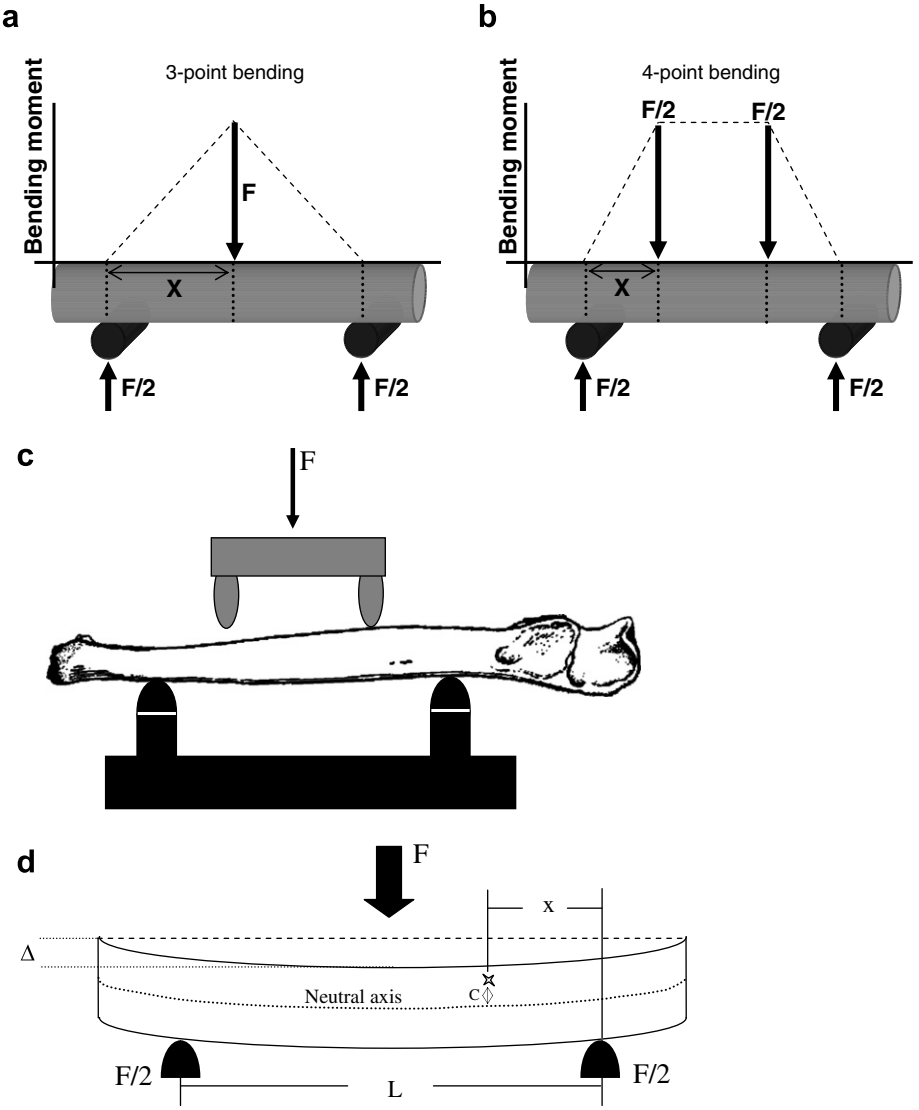

Fig. 10. (a) 3-point bending. The dotted lines depict the magnitude of the bending moment, which increases from 0 at the bottom supports to a maximum value at the mid-point. (b) 4-point bending. The dotted lines depict the magnitude of the bending moment, which is constant within the entire region between the two load-applying prongs. (c) 4-point bending of a whole bone. It can be seen that the 2-pronged loading part will not contact the bone symmetrically due to the uneven contour of the bone. (d) 3-point bending experiment.

maximal load occurs at the point of load application, and the bone will ultimately fracture at this location.

The alternative 4-point bending method is similar except that the load is applied by two loading prongs located equidistance from the mid point (see Fig. 10b). The main advantage of this method lies in the fact that the entire section of bone between these two load-applying prongs is subjected to a uniform moment. In this testing configuration the beam is loaded in pure bending, all strains are in the axial direction, and there is no shear. Nevertheless, bones are mostly tested in 3-point bending, since their irregular surface geometry creates difficulty in having both prongs contact the bone simultaneously (see Fig. 10c). It should be noted that a swivelling upper anvil helps partially overcome this problem.

The experimental procedure involves the measurement of the deflection of the bone at the point of load application and the concurrent measurement of the load, yielding a force–deflection graph. Parameters obtained from this graph include whole-bone stiffness (defined as the slope of the early, linear portion of the load–deflection curve), yield point, maximal load and fracture load (see the parameters specified in parentheses in Fig. 5).

It is also possible to obtain a rough estimate of the Young's modulus of the material from the geometry of the loading device and the measured stiffness of the bone. Such an estimate is based on beam theory and the approximation of the shaft of the tested bone as a uniform hollow tube. The following is a short description of this calculation.

In a 3-point bending setup (see Fig. 10d) the moment at distance x from one of the supports is equal to:

$$M = \frac{F}{2}(L - x) \tag{6}$$

where F is the force applied, and L is the distance between the two bottom supports (see Fig. 10d). At the mid-point between the lower supports x is equal to $\frac{L}{2}$, therefore at that location

$$M = \frac{F \cdot L}{4} \tag{7}$$

Based on beam theory, at the location of load application the strain along the beam ε can be expressed as

$$\epsilon = \frac{12 \cdot c}{L^2} \cdot \Delta \tag{8}$$

where Δ represents the vertical displacement of the bone at the point of load application and c is the distance from the neutral axis (see Fig. 10d).

Making use of Hooke's law (see Eq. (2)) and the equation describing the bending stress (Eq. (3)) we get:

$$E = \frac{\sigma}{\epsilon} = \frac{F \cdot L^3}{48 \cdot I\Delta} \tag{9}$$

Thus one can determine $\frac{F}{\Delta}$ from the load–displacement curve determined in the bending experiment, calculate I and measure L from the geometry of the bone and testing setup, respectively, and obtain an estimate for E. It should be noted though that this method of determining materials property is very coarse, and results can be considered as first approximations only. This is due to the fact the calculation ignores the inhomogeneity and anisotropy of the material, and its complex geometric shape (which is different to a circular hollow tube). Nevertheless, this is a commonly used method to estimate the mechanical properties of the material bone within the whole bone.

Torsion

Torsional testing of whole bone is accomplished by firmly embedding the epiphyseal ends of the tested bone in rectangular or cylindrical blocks of plastic material which are fitted into the grips of the torsion testing machine. Using one of several available testing devices, a torque (twisting moment) is applied to one of these grips while the other is kept firm, and load and angular deformation are recorded. This setup allows the approximate determination of the shear modulus of bone.

Impact loading

The simulation of trauma-associated loading conditions requires high strain rates and is very important in the prediction of bone behaviour under sudden loads in non-physiological directions (i.e. falling). This fact stimulated the development of a class of impact-type loading devices, such as pendulum loading, which uses a hammer of precisely known weight which is dropped from a known height (thus its potential energy is known) and hits the sample in impact; such experiments can yield information on the resistance of whole bones to impact loading at various configurations.

Conclusions

Bone is a composite hierarchical material, therefore investigation of the relationship between the materials properties and the geometry and mechanical behaviour of whole bone is challenging and very complicated. A thorough understanding of this relationship is of importance to clinicians and researchers alike; it helps to understand the normal behaviour of whole bones during physiological loading, identifies areas of peak stresses which are more likely to fracture during intense activity, and allows the prediction of effects of various pathological processes and drug treatments.

Diverse mechanical testing methods (such as bending, torsion and impact loading) have been used to try to describe this relationship, however due to the inherent limitations of these methods, as described in this manuscript, thorough understanding of these relationships has proven elusive, and it is still impossible to predict accurately the mechanical performance of whole bones. In the second part of this manuscript we shall explore novel optical metrology techniques which might help elucidate more precisely and accurately whole-bone response to load.

References

Ammann, P., Robin, B., Riszoli, R., 2003. Long-term exposure to strontium ranelate dose-dependently increases intrinsic bone quality. Journal of Bone and Mineral Research 18, S276.

Burr, D.B., Milgrom, C., Fyhrie, D., Forwood, M., Nyska, M., Finestone, A., Hoshaw, S., Saiag, E., Simkin, A., 1996. In vivo measurement of human tibial strains during vigorous activity. Bone 18, 405–410.

Cowin, S.C., 2001. Bone Mechanics Handbook. CRC Press, Florida, USA.

Currey, J.D., 1988. Strain rate and mineral-content in fracture models of bone. Journal of Orthopaedic Research 6, 32–38.

Currey, J.D., 2002. Bones: Structure and Mechanics. Princeton University Press, Oxford, UK.

Davies, H.M.S., 2005. Peak strains in equine locomotion. Bone 36, S193–S194.

Delmas, P.D., Tracy, R.P., Riggs, B.L., Mann, K.G., 1984. identification of the noncollagenous proteins of bovine bone by two-dimensional gel-electrophoresis. Calcified Tissue International 36, 308–316.

Frasca, P., 1981. Scanning-electron microscopy studies of ground substance in the cement lines, resting lines, hypercalcified rings and reversal lines of human cortical bone. Acta Anatomica 109, 115–121.

Fratzl, P., Schreiber, S., Boyde, A., 1996. Characterisation of bone mineral crystals in horse radius by small-angle X-ray scattering. Calcified Tissue International 58, 341–346.

Fung, Y.C., Tong, P., 2001. Classical and Computational Solid Mechanics. World scientific Publishing Co. Pte. Ltd., Singapore.

Gao, H.J., 2006. Application of fracture mechanics concepts to hierarchical biomechanics of bone and bone-like materials. International Journal of Fracture 138, 101–137.

Hodge, A.J., Petruska, J.A., 1963. Recent studies with the electron microscope on ordered aggregates of the tropocollagen molecule. In:

Ramachandran (Ed.), Aspects of Protein Structure. Academic Press, New York, pp. 289–300.

Judex, S., Lei, X., Han, D., Rubin, C., 2007. Low-magnitude mechanical signals that stimulate bone formation in the ovariectomised rat are dependent on the applied frequency but not on the strain magnitude. Journal of Biomechanics 40, 1333–1339.

Lane, N.E., Yao, W., Balooch, M., Nalla, R.K., Balooch, G., Habelitz, S., Kinney, J.H., Bonewald, L.F., 2006. Glucocorticoid-treated mice have localised changes in trabecular bone material properties and osteocyte lacunar size that are not observed in placebo-treated or estrogen-deficient mice. Journal of Bone and Mineral Research 21, 466–476.

Martin, T.J., Seeman, E., 2007. New mechanisms and targets in the treatment of bone fragility. Clinical Science 112, 77–91.

Martin, R.B., Burr, D.B., Sharkey, N.A., 1998. Skeletal Tissue Mechanics. Springer-Verlag, New York, USA.

Mayer, G., 2005. Rigid biological systems as models for synthetic composites. Science 310, 1144–1147.

Milgrom, C., Finestone, A., Hamel, A., Mandes, V., Burr, D., Sharkey, N., 2004. A comparison of bone strain measurements at anatomically relevant sites using surface gauges versus strain gauged bone staples. Journal of Biomechanics 37, 947–952.

Robling, A.G., Burr, D.B., Turner, C.H., 2001. Recovery periods restore mechanosensitivity to dynamically loaded bone. Journal of Experimental Biology 204, 3389–3399.

Rubin, C.T., Lanyon, L.E., 1985. Regulation of bone mass by mechanical strain magnitude. Calcified Tissue International 37, 411–417.

Schaffler, M.B., Radin, E.L., Burr, D.B., 1989. Mechanical and morphological effects of strain rate on fatigue of compact-bone. Bone 10, 207–214.

Silva, M.J., Brodt, M.D., Hucker, W.J., 2005. Finite element analysis of the mouse tibia: Estimating endocortical strain during three-point bending in SAMP6 osteoporotic mice. Anatomical Record Part A – Discoveries in Molecular Cellular and Evolutionary Biology 283A, 380–390.

Suresh, S., 2001. Graded materials for resistance to contact deformation and damage. Science 292, 2447–2451.

Taylor, D., Lee, T.C., 2003. Microdamage and mechanical behaviour: predicting failure and remodelling in compact bone. Journal of Anatomy 203, 203–211.

Turner, C.H., 2006. Bone strength: current concepts. Annals of the New York Academy of Sciences 1068, 429–446.

Warden, S.J., Hurst, J.A., Sanders, M.S., Turner, C.H., Burr, D.B., Li, J.L., 2005. Bone adaptation to a mechanical loading program significantly increases skeletal fatigue resistance. Journal of Bone and Mineral Research 20, 809–816.

Weiner, S., Wagner, H.D., 1998. The material bone: structure–mechanical function relations. Annals Review Mathematical Science 28, 271–298.

Weiner, S., Traub, W., Wagner, H.D., 1999. Lamellar bone: structure–function relations. Journal of Structural Biology 126, 241–255.